LUBRICATED TRANSPORT OF VISCOUS MATERIALS

Lecture presented at IUTAM conference on lubricated transport of viscous materials, Tobago, Jan. 7, 1997.

DANIEL D. JOSEPH
University of Minnesota
Department of Aerospace Engineering & Mechanics
107 Akerman Hall, 110 Union Street
Minneapolis, MN 55455

Contents

1. Phase arrangements

In two phase flows the dynamic response is tied to the way the phases are arranged. Many configurations are realized in practice; these are often described by flow charts for

- Liquid-liquid
- Gas-Liquid
- Liquid-Solid

In figure 1 you see a cartoon of flow types in oil-water flows. A flow chart for gas-liquid flows is shown in figure 2. There are definitely flow types in liquid-solid flows (figure 3), but as far as I know, flow charts have not yet been prepared for liquid-solid flows.

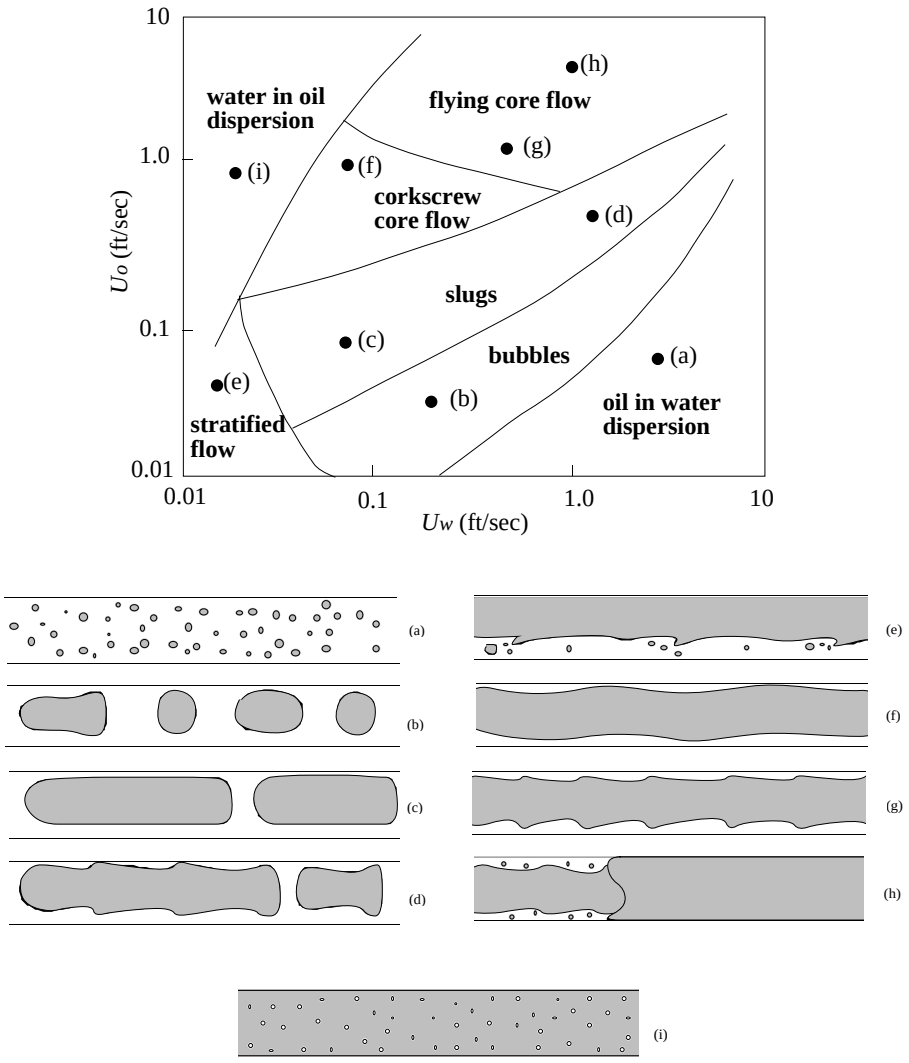

Figure 1. (Joseph, *et al.*, 1997) Cartoons of a flow chart and flow types in horizontal flow when the oil is lighter. The flow is from right to left. All flows but (e) and (i) are lubricated. The holdup ratio $h = \overline{U}_0/\overline{U}_w$ where $\overline{U}_0$ is the average oil velocity and $\overline{U}_w$ is the average water velocity. $h = 1$ for finely dispersed flow like (i), $h = 2$ for perfect core flow, $h \approx 1.5$ for wavy flow.

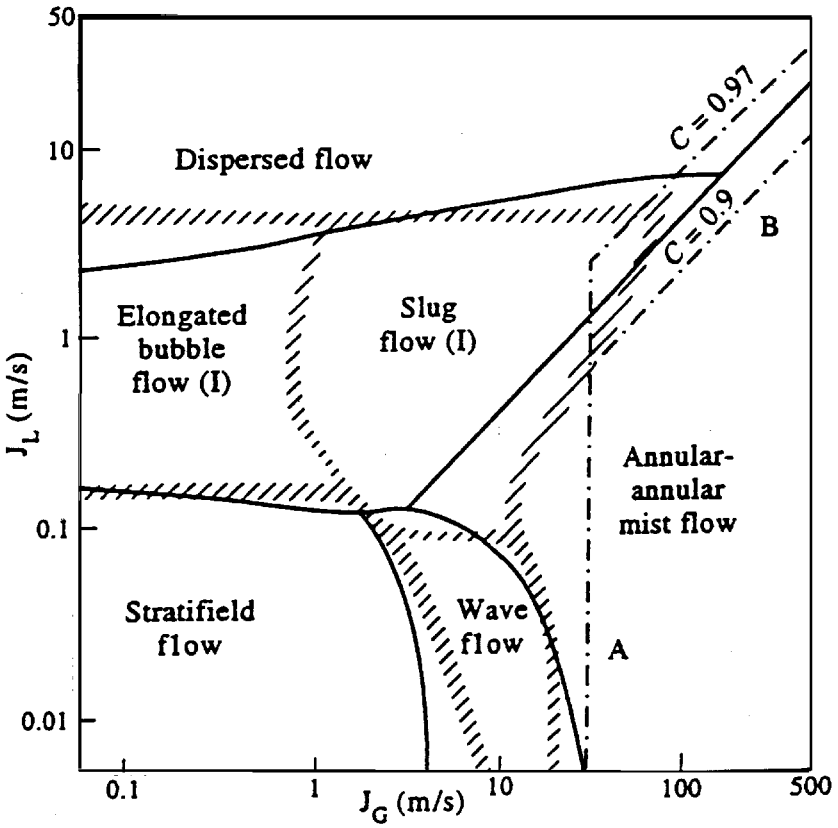

Figure 2. (Joseph, Bannwart and Liu, 1996) Taitel and Dukler's (1976) flow map of horizontal air-water flow at 1 bar and 25°C. The pipe diameter is 25 mm. The solid lines stand for the theoretical transitions proposed by Taitel and Dukler. The dashed lines indicated the experimental diagram of Mandhane, Gregory and Aziz (1974). $\mu_{eff,G} = \mu_{eff,L}$ on the dashed-dot line.

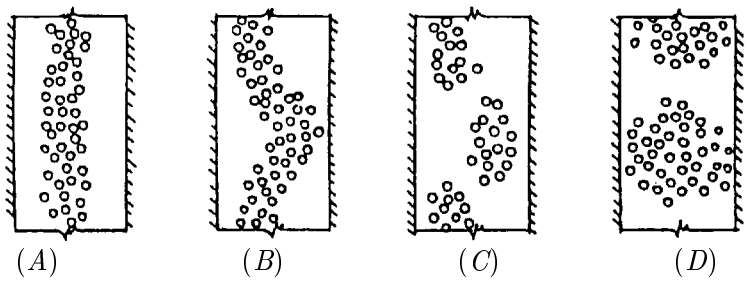

Figure 3. (Brandt and Bugliarello, 1996) Two-dimensional shear flow of neutrally bouyant rigid spheres. Development of instabilities. (*A*) Concentrated Core; (*B*) waves; (*C*) separation; (*D*) discontinuous flow.

2. Types of lubricated flows

- Solids lubricated by liquids.
  - journal bearing
  - pneumatic tube
  - coal log (Henry Lui)
- Lubricate a very viscous liquid with a mobile liquid, say water
  - core flow
  - rollers (figure 4, Joseph *et al.*, 1986)

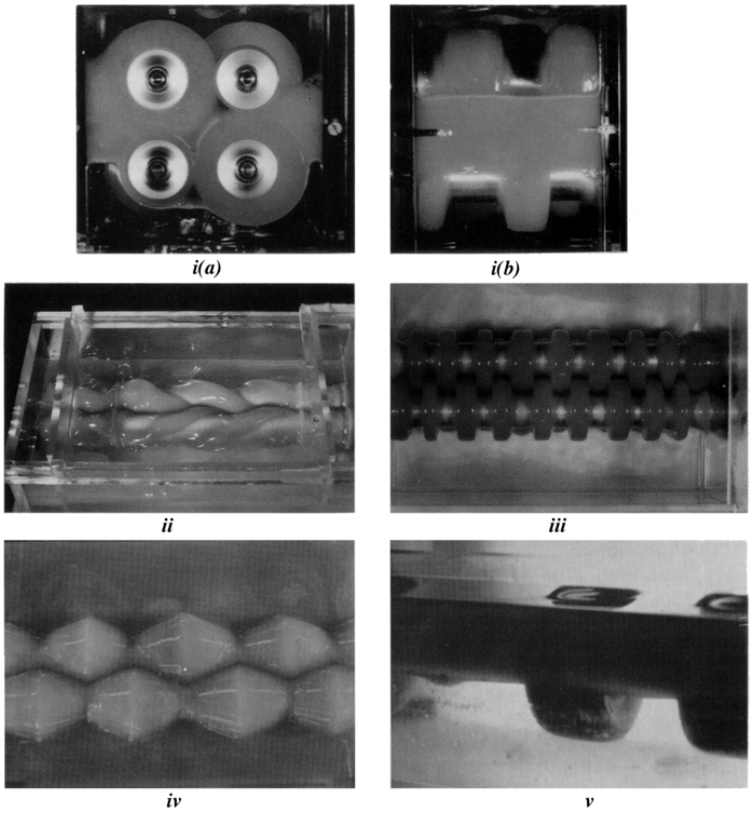

Figure 4. (Joseph *et al.*, 1986) Rollers. STP rotating in water, lubricated all around. The rollers rotate as a rigid body because they are lubricated. You would think they are solids, but they collapse when the motor is turned off. It is amusing to think that we can create an effective solid from a fluid by lubrication.

– Lubricate slurries with water (the particles can't be too heavy or the flow too slow). The water migrates to the wall and the solids to the core (figure 3). Lubricated heavy oil in water emulsions (Orimulsions, Nez *et al.*, 1996).
– Lubricate turbulent gas (high eddy viscosity) with water. Annular gas-liquid flow in horizontal pipes (figure 5) and up-flow.

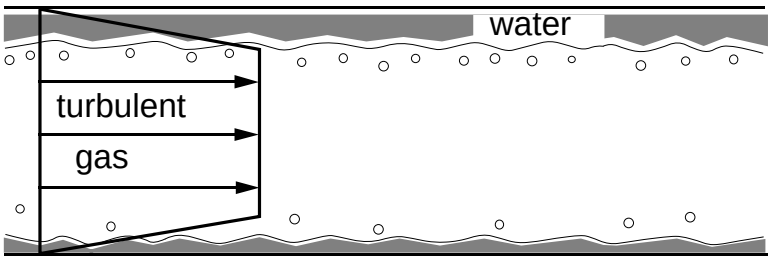

Figure 5. Horizontal annular gas-liquid flow gets stable when the eddy viscosity in the gas gets to be as large as the water ($\cdot - \cdot - \cdot$ line of Joseph, Bannwart and Liu (1996) in figure 2).

– Lubricate turbulent gas in up-flow with a concentrated dispersion of solids raining down pipe walls (figure 6). The gas core is again stabilized by an increase in the eddy viscosity of gas beyond the effective viscosity of the compacted solids. In lubricated slurries particles go to the core, just the opposite.

3. Lubricated pipelining of heavy oil

– Water will go to the pipe wall if the oil viscocity is larger than about 5 poise.
– Drag reductions of the order of the viscocity ratio are possible

$$\mu_0/\mu_w = 1000/\tfrac{1}{100} = 10^5$$

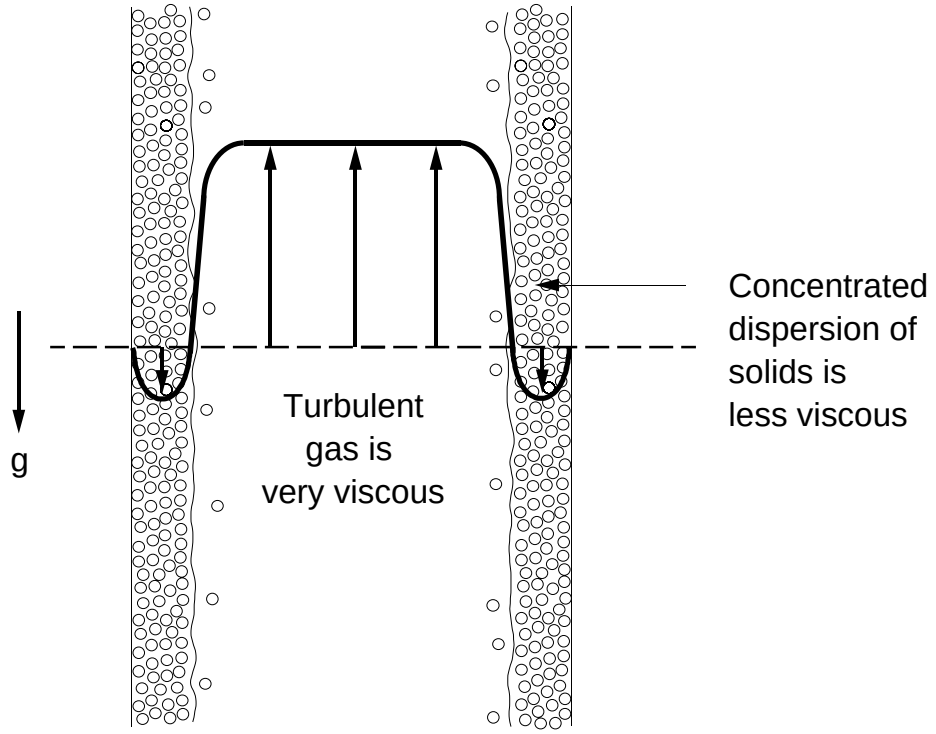

Figure 6. (Joseph, Bannwart and Lui, 1996) Annular solid-gas flow. It is strange to think concentrated solids on the wall have less viscosity than the turbulent gas and that the solids are a lubricant as is suggested by theory (Iske *et al.*, 1995; Joseph, Bannwart and Lui, 1996)

3.1. HISTORY (SEE JOSEPH AND RENARDY, 1992, JOSEPH *ET AL.*, 1996)

1906 Isaacs and Speed proposed to rifle the pipe and throw the water to the wall by centripetal acceleration
1930's Various oil companies built short pilot lines, a few miles
1960's Canadian studies at Alberta by Govier, Hodgson, Charles
1970 - 1982 Shell ran a commercial $8''$ line from Bakersfield to the upgrading facility at ten section. Ran especially well when using produced water, but you got lubrication only for flow velocities

$$U > 3 \text{ ft/sec}$$

You need inertia to levitate the flow
1996 Syncrude froth pilot: This is a 1 km long $24''$ pipe. You get self-lubrication rather than lubrication because the water is already there.

The water is a colloidal dispersion of clay which promotes the self lubrication. Additional water is not added.

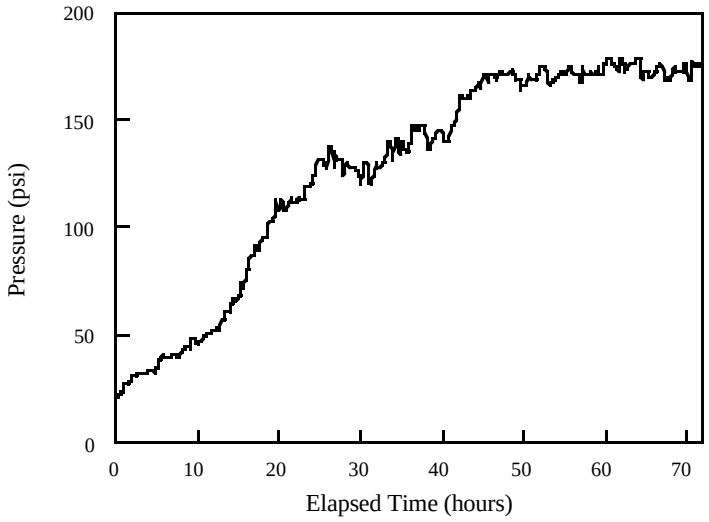

Figure 7. (Joseph *et al.*, 1996) Fouling of the San Tomé test loop with Zuata crude. input fraction = 4%, superficial oil velocity = 1.5 m/sec. Pressure losses increase monotonically as the pipeline fouls. High blockage was experienced after 2 1/2 days of operation.

3.2. FOULING

This is a serious problem for some oils and pipe walls. Venezuelan oils have a high concnetration of asphaltenes which are apt to stick to carbon steel pipes. This problem has so far frustrated the development of commercial lubrication in Venezuela (figure 7). Research in anti-fouling has been carried out with cement-lined and polymeric-lined pipes.

3.3. TURBULENCE

Figure 8 gives friction factor vs. Reynolds number (λ vs. $\mathbb{R}$ defined in Arney *et al.*, 1993) for all published core flow data. The oil moves nearly as a rigid body; the water is usually turbulent and follows the Blasius correlation $\lambda = 0.316/\mathbb{R}^{0.25}$ for $\mathbb{R} < 10^6$. The scatter on the high side of turbulent water in the gap is due to fouling. You can derive this more or less from a K-E model for pure water, no fitting, assuming a smooth interface (Huang *et al.*, 1994).

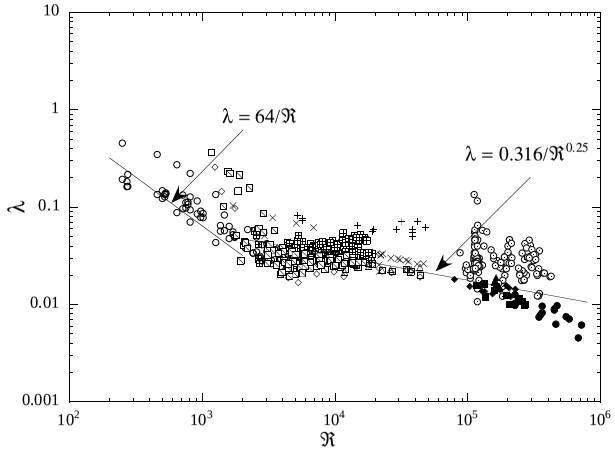

Figure 8. (Arney *et al.*, 1993) Friction factor vs. Reynolds number from different sources.

3.4. CREATION AND ANNIHILATION OF FOULING

The critical cause for concern is the build-up of fouling. In fact most oil will stick to the walls of a carbon steel pipe, but there is no buildup because eventually the oil is torn off the fouled pipe as fast as it is put on. We saw this kind of response in our studies of number 6 fuel oil. There was a layer of oil on the wall, but no build-up of fouling, the pressure drop did not increase.

The same balance between creation and annihilation of fouling occurs for bitumen froth (figure 9).

4. Steep Waves (Joseph and Lui, 1996, Joseph, 1997)

When fluid flows through a gap defined by a wave crest and a solid wall, the pressure at the wave front is much larger than at the rear. This leads to wave steepening at the front side of the wave. This kind of wave steepening appears to be ubiquitous, not only in lubricated transport but also in material processing.

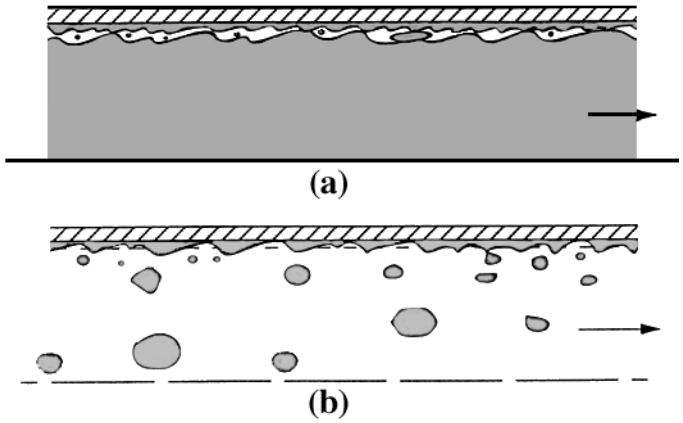

Figure 9. Creation and annihilation of fouling of bitumen froth. The froth is weak because it is covered by clay from clay water and can't stick to itself. The water can coelesce to form a lubricating sheath between the fouled wall and the core. Bits of oil are torn away and new fouling appear to be in balance, since the pressure gradient doesn't increase. You pay a price for fouling approximately 20 times the cost of water alone. You can wash the froth from the pipe with clay water (b); pegging is not required.

4.1. INSTABILITY OF LONGWAVES

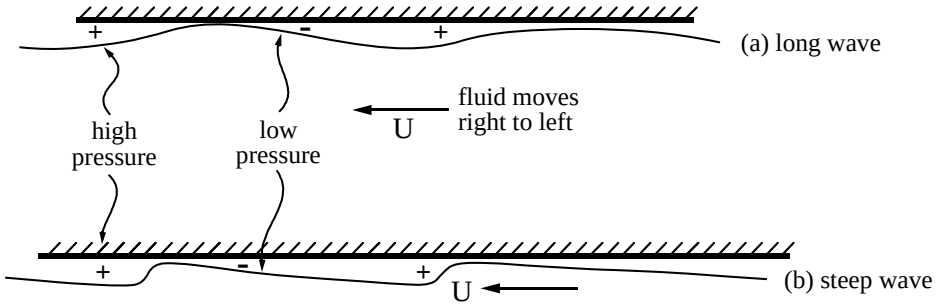

Figure 10. The wave front (a) steepens (b) due to high pressure at the front.

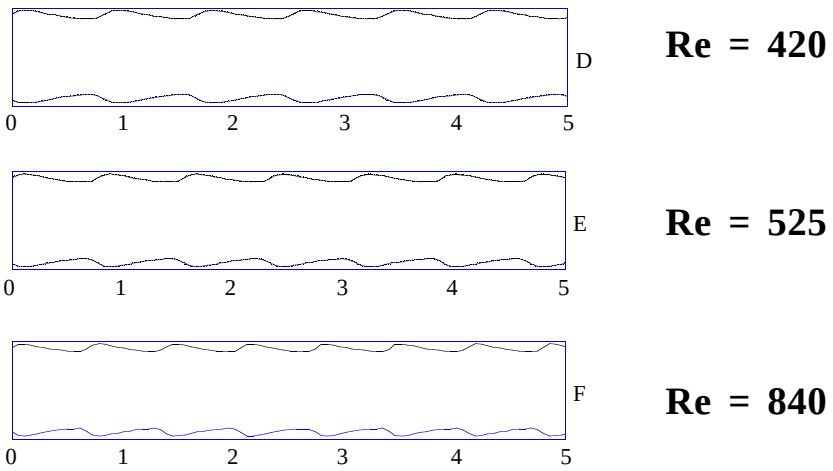

Figure 11. Numerical calculation of Bai *et al.*, (1996) for $[\eta, h] = [0.86, 1.4]$. The wave length shortens and the wave front steepens as the Reynolds number is increased.

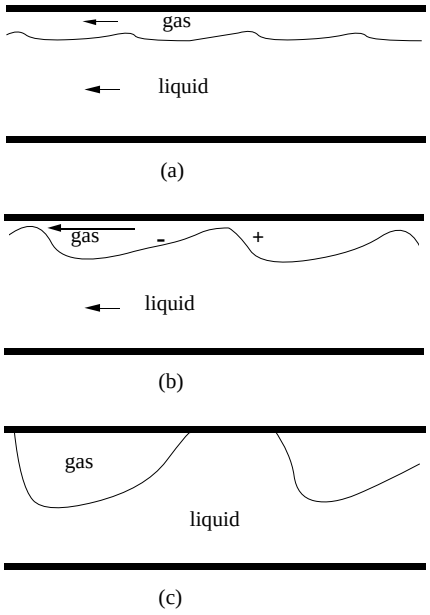

Figure 12. (Joseph *et al.*, 1986) Slugging in gas-liquid flow. The high pressure at the front side steepens the wave and the low pressure at the back side smoothes it. If the amplitude of the wave is large enough it will touch the wall. Bernoulli effects can also suck the liquid to the wall when the gas velocity is large. Note that we have avoided drawing the ripples and small roll waves which are probably always superimposed on the gas-liquid interface. We focus on macro-structures.

4.2. LEVITATION OF A SLIPPER BEARING

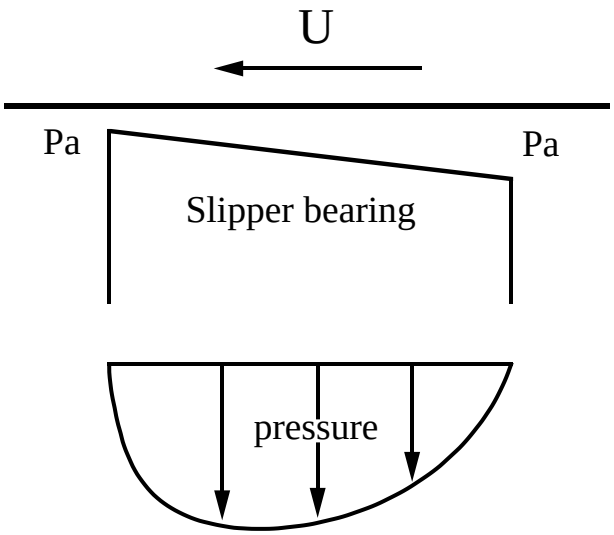

Figure 13. The pressure distribution levitates the bearing. If U is reversed, the slipper bearing will be sucked toward, rather than pushed away from the moving wall.

4.3. LEVITATION OF CORE FLOW

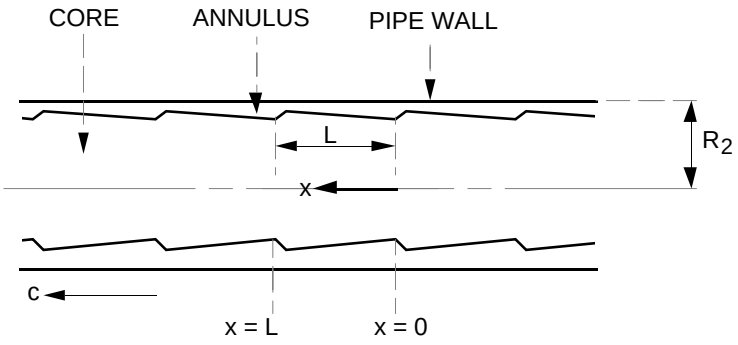

Figure 14. (after Ooms *et al.*, 1984) The core is at rest and the pipe wall moves to the left. The core shape is assumed to be a sequence of slipper-like bearings. This configuration should not levitate in the low Reynolds number of lubrication theory; you get anti-levitation instead, suggesting that inertia is needed for levitation.

4.4. STEEP WAVES IN ANNULAR FLOWS

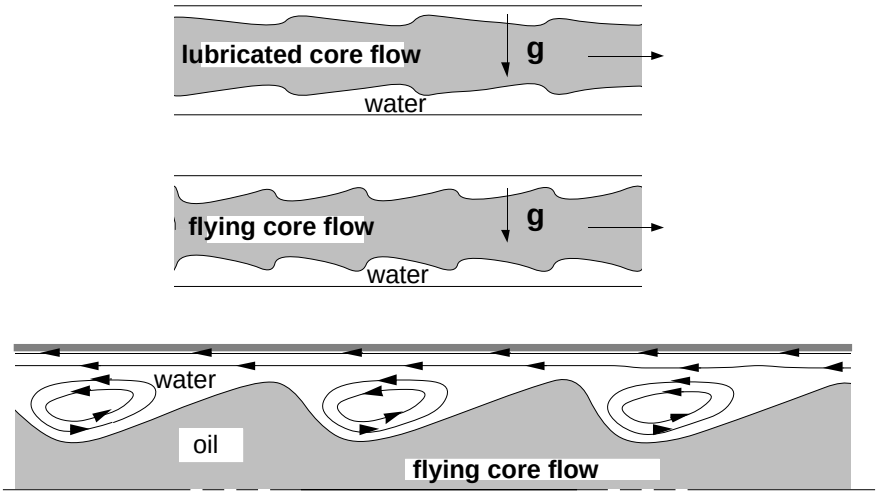

Figure 15. (Feng, *et al.* 1995) (*top*) The interface resembles a slipper bearing with the gentle slope propagating into the water; the shape of these waves is unstable. (*middle*) The high pressure at the front of the wave crest steepens the interface and the low pressure at the back makes the interface less steep. (*bottom*) The pressure distribution in the trough drives one eddy in each trough. The waves in (a) are unstable and lead to (b). To get a lift from this kind of wave it appears that we need inertia, as in flying. Liu's (1982) formula for capsule lift-off in a pipelin in which the critical lift off velocity is proportional to the square root of gravity times the density difference is an inertial criterion. Industrial experience also suggests an inertial criterion, since CAF in the Shell line could be maintained only when the velocity was greater than 3 ft/s; at lower velocities the drag was much greater.

Figure 16. (Joseph, 1997). Core annular flow of #6 fuel. The saw-tooth waves on the oil core in a horizontal pipeline. The flow is from left to right.

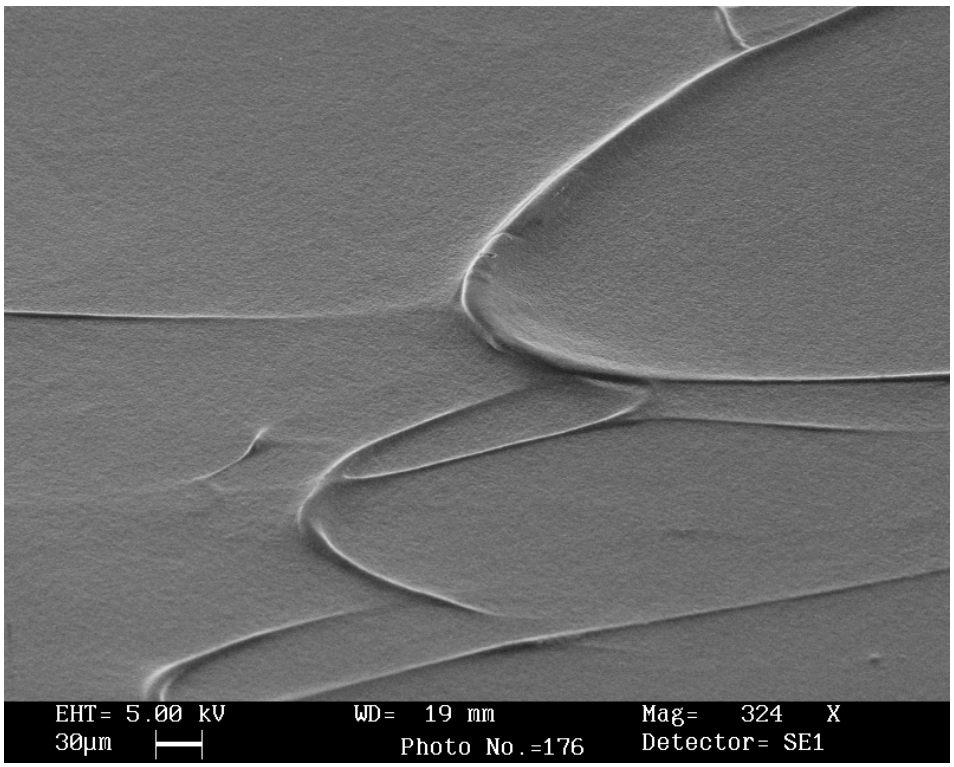

Figure 17. (Joseph, 1997, Courtesy of R.P.G. Rutgers) Film blown of a 40mm Kiefel extruder with a 0.8 mm die gap width and wall shear rate = 277 s^{-1}. Direction of melt flow is right to left. Steep fronts advance.

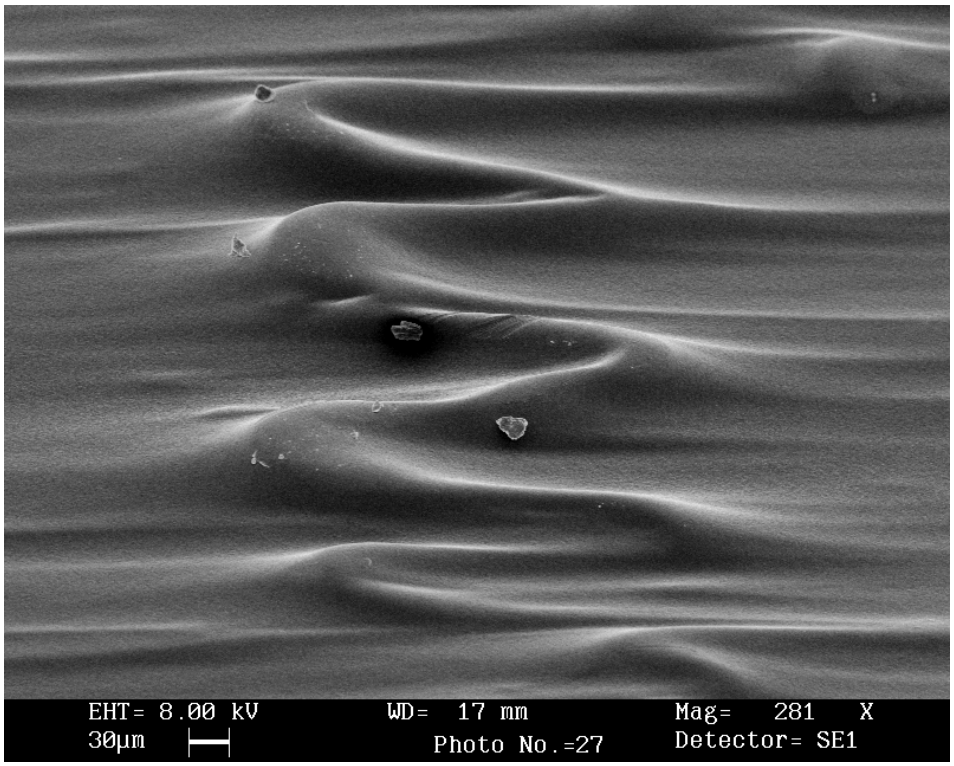

Figure 18. (Courtesy of R.P.G. Rutgers) Extruded tape from a 25 mm Betol single screw extruder with a 15:1 abrupt entry slit die of 1 mm gap width (x), and 8 mm length (z). Haul off ratio of 7.3:1, melt temperature of 178°C, wall shear rate = 163 s^{-1}. The extrudate surface shown is the y-z plane. Direction of flow from right to left. Scale as indicated on the photograph.

5. Elastohydrodynamic Steep Waves Produced by Lubrication Forces in Ultrathin Liquid Films

Figures 22, 23, 24 are photographs of the consequences of ultrathin film lubrication dynamics on the mica boundaries of a surface force apparatus by Israelichvili and co-workers (Kuhl *et al.*, 1994). The boundaries of the thin film are smooth mica. The fluid is polybutadiene $M \approx 10^4, \mu = 180$ poise. Typical values are velocity 10^{-4}cm/sec, gap $h = 2 \times 10^{-6}$cm, $\mathbb{R} \approx 10^{-12}$. This is Stokes flow, but it gives rise to steep waves of mica due to high and low pressures associated with lubrication.

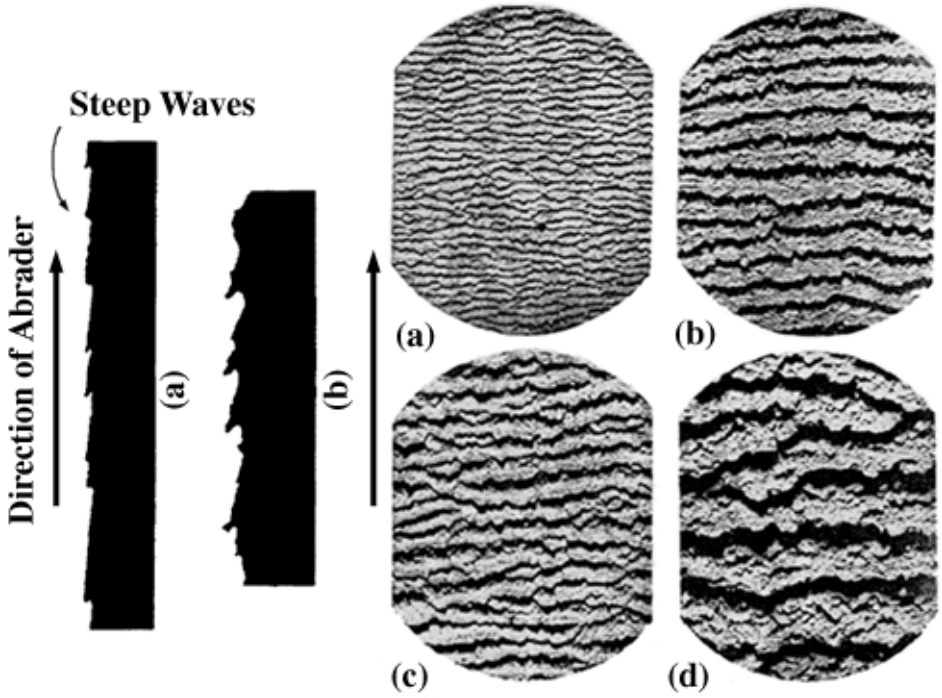

Figure 19. (left): Profiles of abrasion patterns: (a) gum vulcanizate of NR abraded under $1 \cdot 6$ kg/cm^2 on silicon-carbide cloth, $5\times$; (b) worn NR tyre surface, horizontal magn. $30\times$, vertical magn $42 \cdot 5\times$. Trans IRI., 1952, 28, 259, Fig 3.

Figure 20. (right): Abrasion patterns on two black-filled NR vulcanates: (a) and (c) 45 pph HAF; (b) and (d) 25 pph HAF. Tracks: (a) and (b) fine tarmac; (c) and (d) coarse concrete. Direction of abrasion upwards. Magn. 14 $\times$. Wear, 1958, 1, 406, Fig. 17.

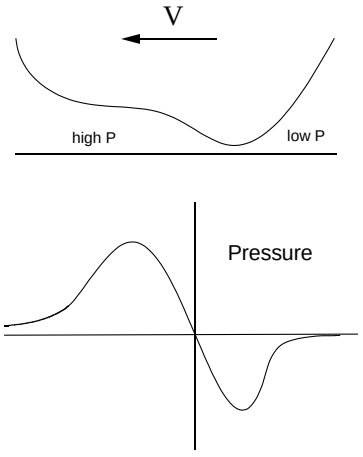

Figure 21. Pressure distribution according to lubrication theory

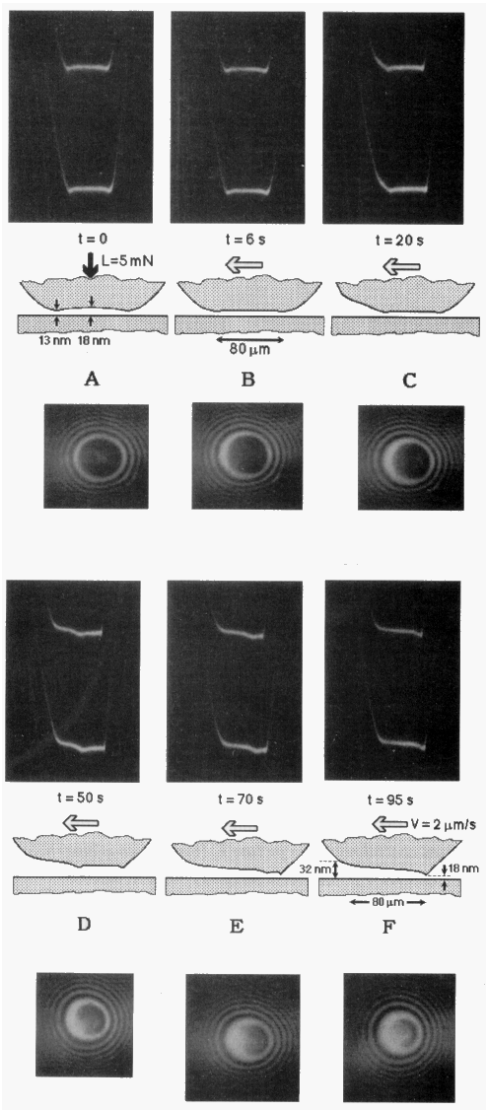

Figure 22. (Kuhl *et al.*, 1994) Development in time of the elastohydrodynamic deformation of shearing surfaces, starting from the profile at rest (A at $t = 0$) and gradually changing to the steady-state profile (F) at a constant sliding velocity of 2μm/sec. In the optical microscope view (bottom) the circular patterns (Newton's rings) arise from constructive interference of monochromatic light. The dark central region is the area of minimum gap separation. The gradually changing film thickness profile as the surfaces reach steady sliding is seen as a changing brightness within the contact zone.

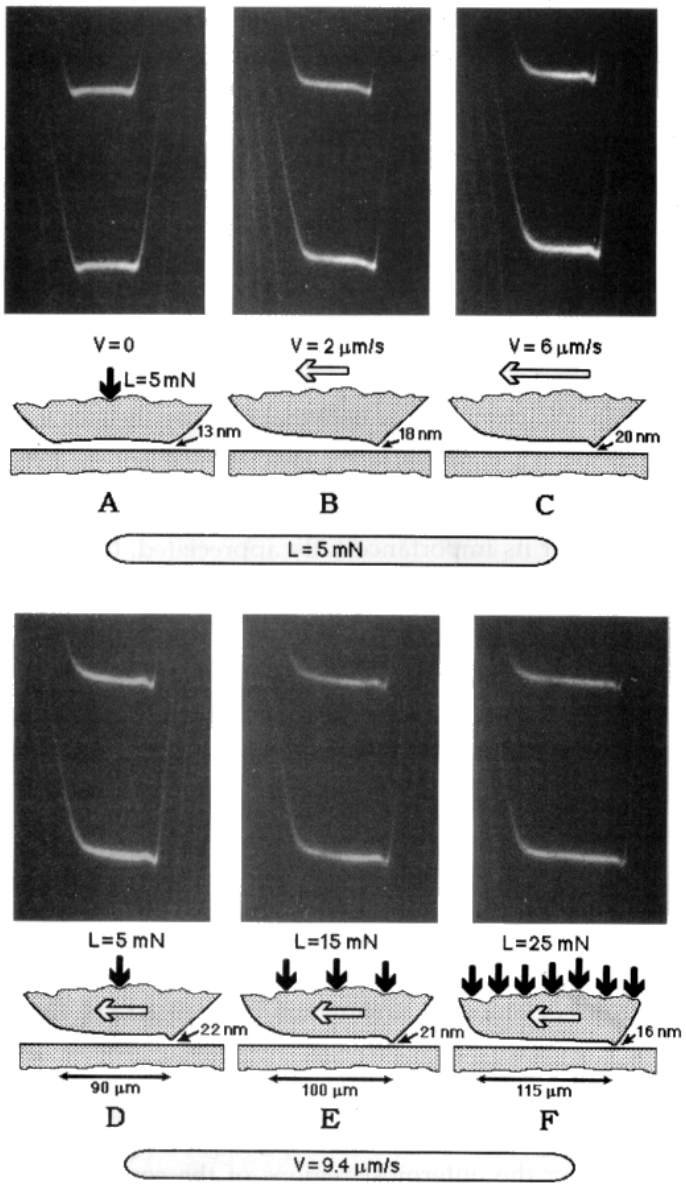

Figure 23. (Kuhl *et al.*, 1994) (A-D) The effect of increasing velocity on surface deformation at constant load L. The deformation of the front edge and the separation of the two surfaces increases with increasing velocity. (D-F) At constant sliding velocity, an increased load decreases the film thickness in the gap and increases the area of contact.

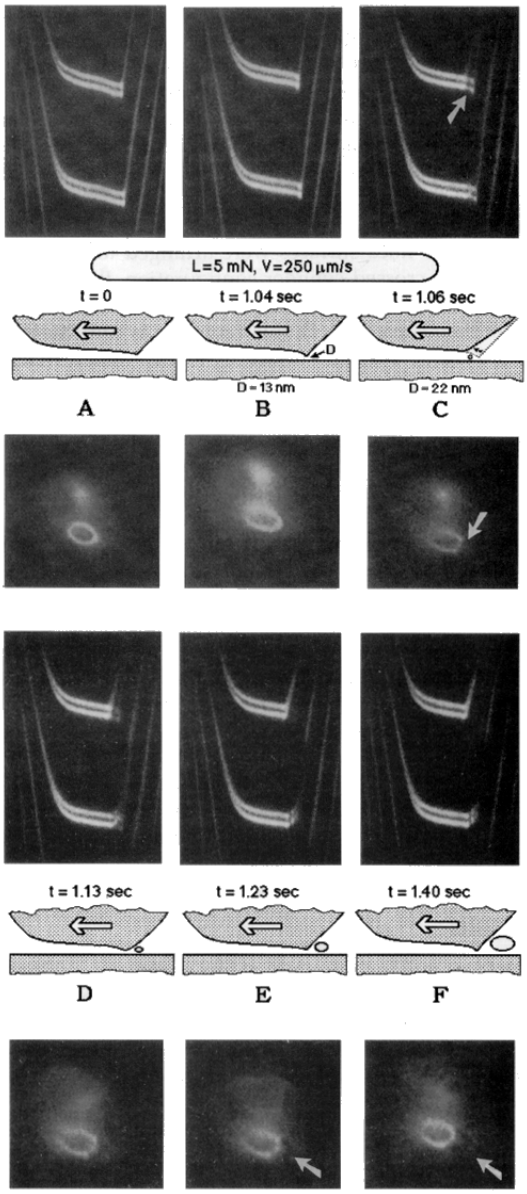

Figure 24. (Kuhl *et al.*, 1994) Surface deformation and formation of a cavity at high sliding velocity, $\eta > \eta_c$. The trailing edge (B) becomes very pointed due to the large tensile stresses developed under high shear rates. A cavity is formed as the surfaces rapidly snap forward (C) to a less deformed shape. Pictures D to F show the evolution and growth of a cavity with time.

6. Melt Fracture

These are cracks, fractures or waves on polymer extrudate, plastics. At low rates of extrusion there is no extrudate distortion; at a critical extrusion the polymer is said to slip. I think that a layer near the wall becomes soft, a lubrication layer (Joseph and Lui, 1996, Joseph, 1997). You see the onset of lubrication as a break in the flow curve.

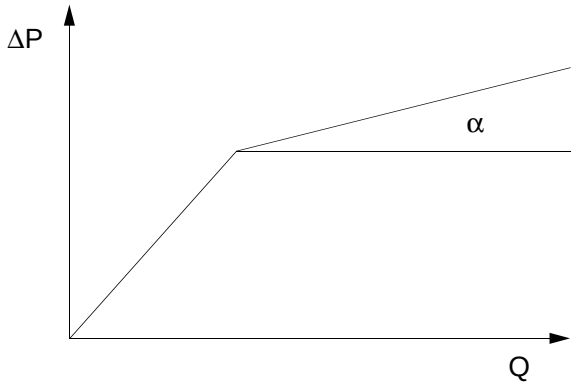

Figure 25. Cartoon of the flux curve given the pressure drop across a capillary versus the volume flux. The frictional resistance decreaces at the point of discontinuity, with the complete slipping when $\alpha = 0$.

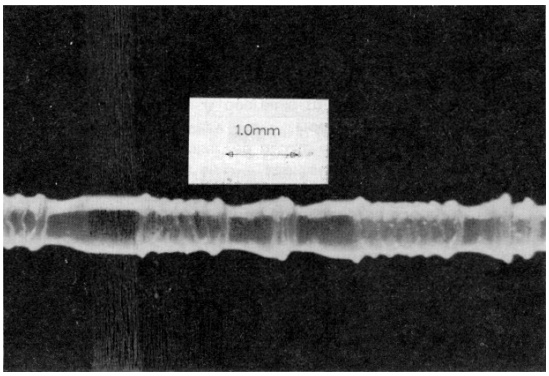

Figure 26. (Kalika and Denn, 1987) Extrusion of LLDPE: Transition region observed in stick-slip flow region $8V/D = 985$, $L/D = 100/1$. The authors do not remember which way the melt was extruded. We guess that the steep wave advances

7. Melt Fracture & Snakeskin

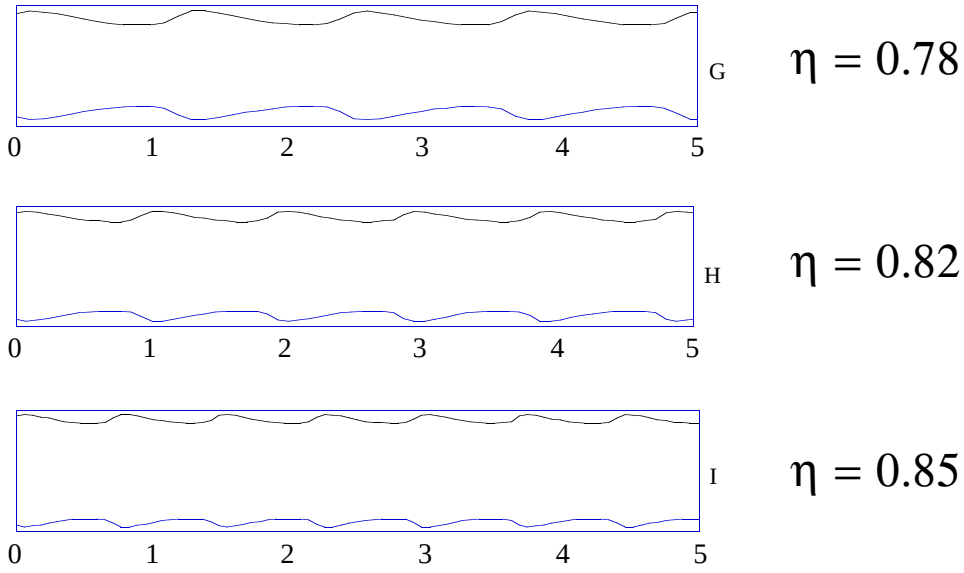

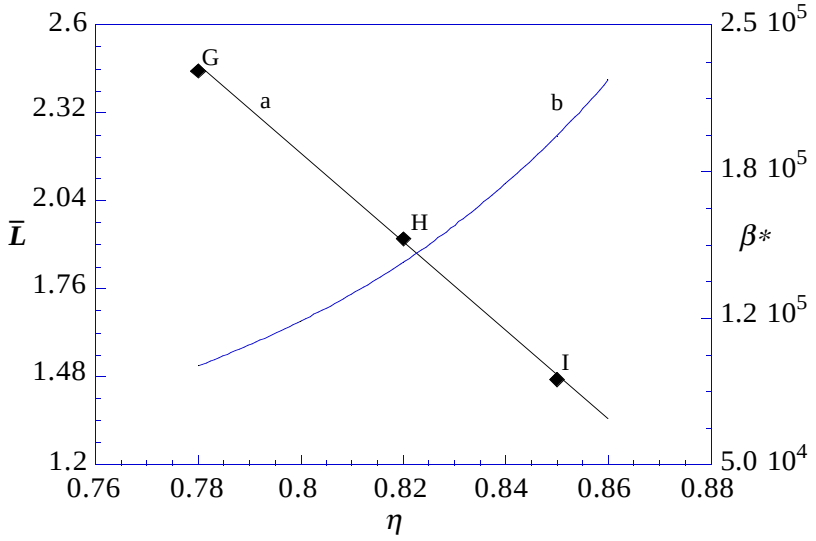

Figure 27. Numerical calculation of Bai, Kelkar and Joseph (1996). Wavelength $\overline{L} = 13.5 - 14.1\eta$ for (IR, h) = (600, 1.4). **The wavelength and amplitude tend together to zero as $\eta \to 1$.** (see Joseph *et al.*, 1997)

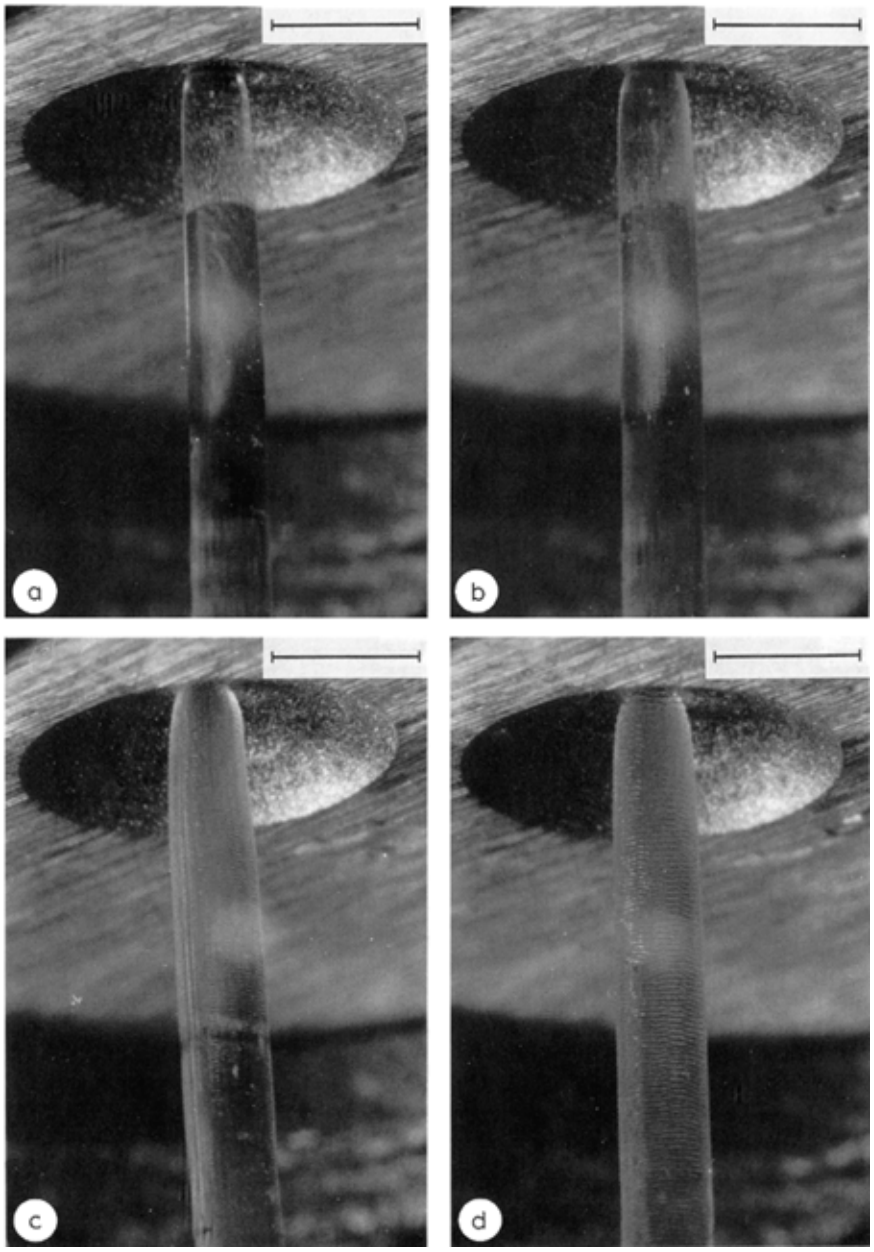

Figure 28. (Piau and Kissi, 1990) The short waves on (b), (c) and (d) are called "sharkskin". On them, and on the larger waves (c) through (b), the steep side advances.

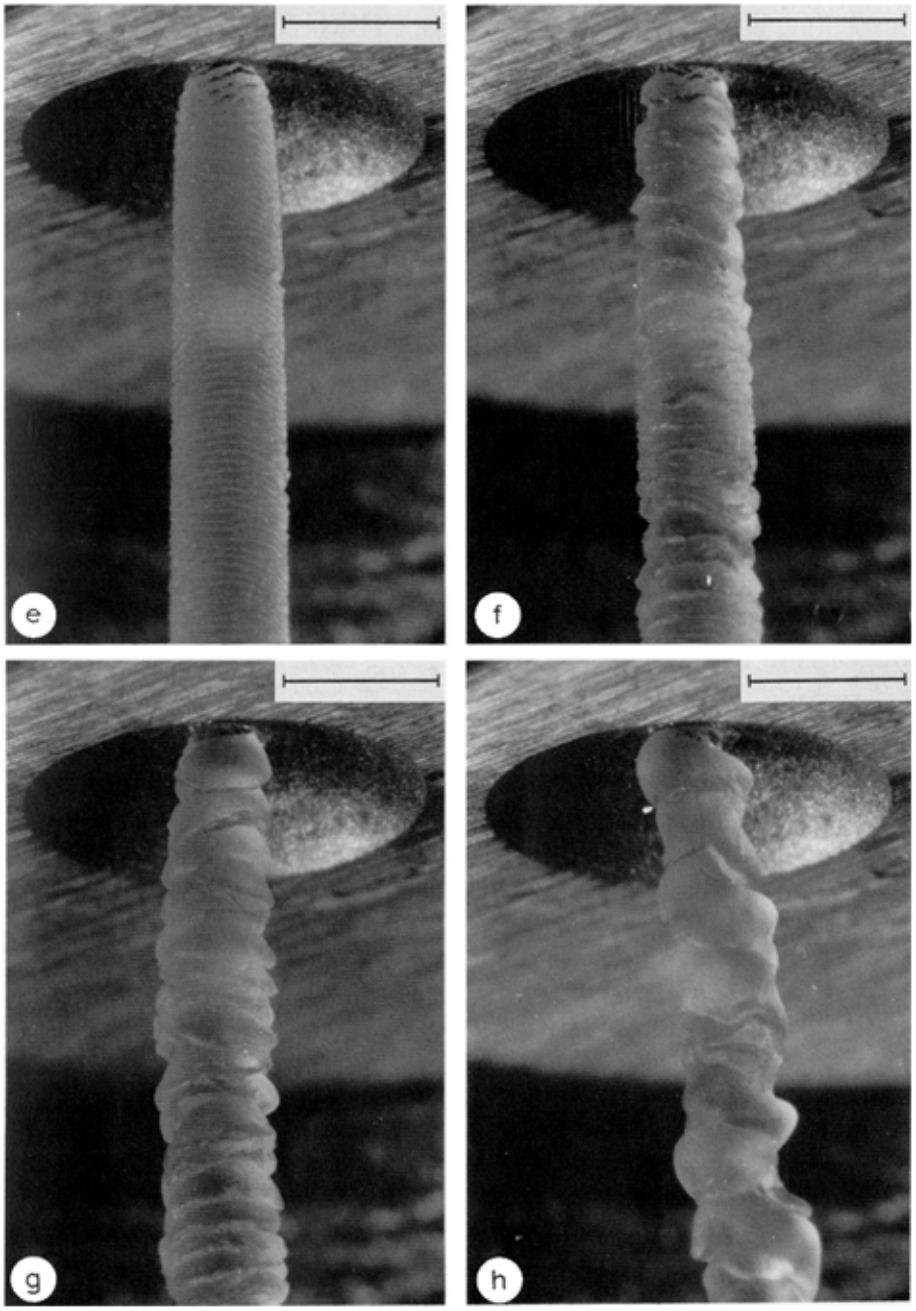

Figure 28, continued.

References

Arney M.S., Bai R., Guevara E., Joseph D.D., Liu K. (1993) Friction factor and holdup studies for lubricated pipelining, *Int. J. Multiphase Flow.*, **19** (6), 1061-1076.

Arney M.S., Ribeiro G.S., Guevara E., Bai R., Joseph D.D. (1995) Cement lined pipes for water lubricated transport of heavy oil, *Int. J. Multiphase Flow,* (In press).

Bai, R., Kelkar K., Joseph D.D. (1996) Direct simulation of interfacial waves in a high viscosity ratio and axisymmetric core annular flow, *J. Fluid Mech*, **327**, 1-34.

Brandt A., Bugliarello G. (1966) Concentration redistribution in the shear flow of monolayers of suspended particles. *Trans. Soc. Rheol.*, **10**(1), 229-251.

Charles M.E. (1963) The pipeline flow of capsules. Part 2: Theoretical analysis of the concentric flow of cylindrical forms, *Can. J. Chem. Engng.*, **46**.

Charles M.E., Govier G.W., Hodgson G.W. (1961) The horizontal pipeline flow of equal density of oil-water mixtures, *Can. J. Chem. Engng.* **39**, 17-36.

Chen, Y., Israelachvili, J., New mechanism of cavitation damage. *Science*, **252**, 1157-1160.

Feng J., Huang P.Y., Joseph D.D. (1995) Dynamic simulation of the motion of capsules in pipelines, *J. Fluid Mech.*, **286**, 201-207.

Huang A., Christodoulou C., Joseph D.D. (1994). Friction factor and holdup studies for lubricated pipelining. Part II: Laminar and k-e models of eccentric core flow, *Int. J. Multiphase Flow*, **20**(3), 481-91.

Issacs J.D., Speed J.B. (1904), U.S. Patent No. 759,374.

Iske P.L., Sergeev Y.A., Boersma W.H., Kurdyumov V.N., Moors J.H.J. (1995) Partical phase boundary layer theory of solid concentration and velocity profiles in circulating fluidized bed risers, in *Proceedings of the 2nd International Conference on Multiphase Flow* '95, Kyoto-Japan, FB1-33-37.

Joseph D.D. (1997) Steep wave fronts on extrudates of polymer melts and solutions: lubrication layers and boundary conditions, *JNNFM.*

Joseph D.D., Bannwart A., Liu J. (1996), Stability of annular flow and slugging, *Int. J. of Multiphase Flow*, **22**(6): 1247-54.

Joseph D.D., Bai R., Chen K.P., Renardy Y.Y. (1997) Core annular flows, **29**.

Joseph D.D., Liu J.Y. (1996) Steep wave fronts on extrudates of polymer melts and solutions. *J. Rheol.*

Joseph D.D., Nguyen K., Beavers G.S. (1986) Rollers, *Physics of Fluids* **29**, 2881.

Joseph D.D., Renardy Y.Y. (1993) Fundamentals of Two-Fluid Dynamics, New York: Springer-Verlag.

Kalika D.S., Denn M.M. (1987) Wall slip and extrudate distortion in linear low-density polyethylene, *J. Rheol.*, **31**, 815-834.

Kuhl, T., Ruths, M., Chen, Y.L., Israelachvili, J., Direct visualization of cavitaion and damage in ultrathin liquid films. *The Journal of Heart Valve Disease*, **3** (suppl. I) 117-127 (1994).

Liu H. (1982) A theory of capsule lift-off in pipeline, *J. Pipelines 2*, 23-33.

Mandhane J.M., Gregory G.A., Aziz K. (1974) A flow pattern map for gas-liquid flow in horizontal pipes, *Int. J. Multiphase Flow*, **1**, 537-553.

Nez G.A., Briceo M., Mata C., Rivas H., Joseph D.D. (1996) Flow characteristics of concentrated emulsions of very viscous oil in water, *J. Rheol.*, (In press).

Ooms G., Segal A., Van der Wees A.J., Meerhoff R., Oliemans R.V.A. (1984) A theoretical model for core-annular flow of a very viscous oil core and a water annulus through a horizontal pipe. *Int. J. Multiphase Flow.* **10**, 41-60.

Piau J.M., Kissi N.E., Tremblay B., Influence of upstream instabilities and wall slip on melt fracture and sharkskin phenomena during silicones extrusions through orifice dies, *J. Non-Newtonian Fluid Mech.*, **34** (1990), 145-80.

Taitel Y., Dukler A.E. (1976), A model for predicting flow regime transitions in horizontal and near horizontal gas-liquid flow, *AIChE J.*, **22**, 47- 55.